

# Theoretical and computational study of the energy dependence of the muon transfer rate from hydrogen to higher- $Z$ gases

Dimitar Bakalov<sup>a,\*</sup>, Andrzej Adamczak<sup>b</sup>, Mihail Stoilov<sup>a</sup>, Andrea Vacchi<sup>c</sup>

<sup>a</sup>*Institute for Nuclear Research and Nuclear Energy, Bulgarian Academy of sciences, Tsarigradsko chaussée 72, Sofia 1784, Bulgaria*

<sup>b</sup>*Institute of Nuclear Physics, Polish Academy of Sciences, ul. Radzikowskiego 152, 31-342 Krakow, Poland*

<sup>c</sup>*Istituto Nazionale di Fisica Nucleare, Sezione di Trieste, Via A. Valerio 2, 34127 Trieste, Italy*

---

## Abstract

The recent PSI Lamb shift experiment and the controversy about proton size revived the interest in measuring the hyperfine splitting in muonic hydrogen as an alternative possibility for comparing ordinary and muonic hydrogen spectroscopy data on proton electromagnetic structure. This measurement critically depends on the energy dependence of the muon transfer rate to heavier gases in the epithermal range. The available data provide only qualitative information, and the theoretical predictions have not been verified. We propose a new method by measurements of the transfer rate in thermalized target at different temperatures, estimate its accuracy and investigate the optimal experimental conditions.

*Keywords:* muonic hydrogen, muon transfer, proton radius, hyperfine structure, laser spectroscopy

---

## 1. Introduction

The laser spectroscopy measurement of the hyperfine structure of the ground state of the muonic hydrogen atom was first proposed more than two decades ago [1], motivated by the understanding that in some sense it would be complementary to the top accuracy measurements of the hyperfine splitting (HFS) in ordinary hydrogen [2]. Subsequent studies revealed, however, some severe difficulties to this goal: the absence of a tunable near-infrared (NIR) laser with sufficient power that necessitates the use of a multi-pass optical cavity to enhance the stimulation of transitions between the hyperfine levels, which in turn makes inapplicable the initially proposed experimental method. In the following

---

\*Corresponding author

years an alternative experimental method was proposed that exploits specific features of the muon transfer reaction at epithermal collision energies [3] and is compatible with the use of a multi-pass cavity. Also, the recent progress in the development of pulsed NIR sources of monochromatic radiation and IR optics [4] has brought the produced laser power close to the needed magnitudes. All this made the experimental project look feasible, though still remaining a significant challenge. What supplied the missing motivation to start the work on the project were the results of the recent muonic hydrogen Lamb shift experiment at PSI [5] and the discovered incompatibility of the values of the charge radius of the proton extracted from muonic hydrogen spectroscopy on the one hand, and ordinary hydrogen spectroscopy and electron-proton scattering data, on the other. The few years of intense search for an explanation of this discrepancy have not lead to any conclusion, and the most direct way to throw light on the subject — next to an independent new measurement of the proton charge radius — appears to be the measurement of the hyperfine splitting in muonic hydrogen and extracting from it the proton Zemach radius: confirming the value obtained from hydrogen spectroscopy would probably give more weight to the explanations supposing methodology uncertainties in the hydrogen-based proton charge radius, while in the opposite case the search for new physics will have good reasons to be intensified.

With this motivation in mind, as a first stage of the preparation for the measurement of the HFS in muonic hydrogen, we started the thorough study of the efficiency and accuracy of the method proposed for this experiment in Ref. [3]. Its physical background is simple: the muonic hydrogen atoms that absorb a photon of the resonance frequency, undergo a hyperfine para-to-ortho transition. When de-excited back to the para spin state in a collision with a  $\text{H}_2$  molecule, these atoms are accelerated by  $\sim 0.1$  eV [3]. The number of atoms that have undergone the above sequence (and therefore — the tuning of the laser to the resonance hyperfine transition frequency) can be determined by observing a reaction whose rate depends on the energy of the  $\mu^-p$  atoms. In Ref. [3] it was proposed to observe the transfer of the muon from muonic hydrogen to the nucleus of a heavier gas added to the hydrogen target for which the transfer rate is energy-dependent in the epithermal range. There are experimental evidences that for some gases (e.g., oxygen, argon, etc.) this is indeed the case [6, 7, 8]. The goal of our investigations is to obtain reliable quantitative data on the energy dependence of the rate of muon transfer to these gases — and possibly other as well — in order to select the optimal chemical composition and physical parameters (pressure, temperature) of the hydrogen gas target that will provide the highest accuracy in the future measurements of the hyperfine splitting of  $(\mu^-p)_{1s}$  and the Zemach radius of the proton. In the present paper we focus at the main physical processes with  $\mu^-p$  atoms in a mixture of hydrogen and a higher- $Z$  gas, and deduce the optimal experimental conditions for the measurement of the energy dependence of the muon transfer rate to the admixture gas. The results have been obtained with a Monte Carlo simulation code that uses the cross sections and rates for the scattering  $\mu^-p+\text{H}_2$ , which were calculated in Refs. [9, 10]. The code has been verified on the many

preceding occasions (see, e.g., [8, 11, 12]).

## 2. Preceding results and novelty of the proposed measurements

The muon transfer in collisions of muonic hydrogen atoms with atoms of higher-Z gas admixtures has been actively investigated for many years because of the important impact of hydrogen impurities on the observable rates of specific reactions such as nuclear muon capture [13], muonic molecule formation [14], etc. In the limit of low collision energies, theory predicts in the lowest order approximation a flat energy dependence of the muon transfer rate [15, 16], while more refined calculations show that for some gases its value may vary by up to an order of magnitude for collision energies below 1 eV [17]. Some experimental data, e.g., on transfer to sulfur [6], consist of a single data point, the average rate of muon transfer at certain pressure and temperature, obtained as the disappearance rate of muonic hydrogen atoms and determined from the time distribution of the events of de-excitation of the muonic atoms of the heavier gas. In the case of oxygen [6], argon [8] and neon [7], however, the time distributions of these events clearly display two different time ranges with substantially different disappearance exponents for the hot and the thermalized atoms. This was interpreted as an evidence for a non-flat energy dependence of the muon transfer rate [11], and a step-function was introduced to describe qualitatively the energy dependence of the transfer rate to oxygen, argon and neon. The earlier estimates of the efficiency of the experimental method in [1, 3] were obtained using this step-function approximation. Its accuracy, however, is far from what is needed for the planning and optimization of the muonic hydrogen hyperfine experiment because the contribution from the atoms with energies in the whole epithermal range is averaged over their energy distribution and is accounted for with a single parameter — the disappearance slope for the “unexpected delayed” events [6] — which incorporates the uncertainties due to the strongly model-dependent energy distribution of the epithermal atoms [18, 19, 20]. To solve the problem, we propose to perform instead a series of measurements of the muon transfer rate from *thermalized muonic hydrogen atoms* at different temperatures in an as broad as possible temperature range. The numerical technique of investigating the energy dependence of the muon transfer rate, which is presented in Sect. 4, relies substantially on the assumption that the muonic hydrogen atoms are thermalized and their energy distribution — the Maxwell-Boltzmann distribution — contains no uncertainties. Our study in Sect. 3 is also focused on the processes in a mixture of hydrogen and higher-Z gases at thermal equilibrium.

## 3. Processes involving the muonic hydrogen atoms in a mixture of hydrogen and higher-Z gases

When slowed down and stopped in a mixture of hydrogen and higher-Z gases, a negative muon is captured by the Coulomb field of the nuclei and forms exotic muonic atoms in which one (or more) of the electrons are ejected and

replaced by the muon. We do not consider here the processes of muon capture in an excited state of the exotic atom and the subsequent de-excitation by competing Auger and radiative transitions and in non-elastic collisions because for the hydrogen target densities of interest (pressures above 10 atm at room temperature) the whole cascade down to the ground  $1s$  state takes no more than about 1 ns. This choice of the target density is determined by the specific features of the available gas containers: simulations (to be reported elsewhere) with the FLUKA code [21] have shown that too few muons are stopped in the target at lower densities. So, to a good approximation, the description of the history of a muonic atom can start from the ground  $1s$  state.

In the general case (when the target gas is a natural mixture of hydrogen and deuterium), the following processes take place: elastic scattering of the muonic atoms, spin-flip, muon exchange between the hydrogen isotopes, and rotational-vibrational transitions in target molecules; formation of the  $pp\mu$ ,  $pd\mu$ , and  $dd\mu$  molecules; nuclear fusion in  $pd\mu$  and  $dd\mu$ ; nuclear muon capture; muon decay, and muon transfer from muonic hydrogen atoms to atomic states of higher- $Z$  elements. The part of muons that are transferred to muonic deuterium at natural deuterium concentration is small and has little impact on the process of muon transfer to higher- $Z$  nuclei [22]; nuclear fusion therefore can also be neglected. The muons that are captured in muonic molecules drop out of the sequence of processes leading to transfer to higher- $Z$  gases; since muonic molecule formation [14] is much slower than muon transfer even at low admixture gas concentration (see Sect. 3.3) it will not be taken into account. As for the muons directly captured in muonic atoms of the higher- $Z$  admixture gas, their fast cascade de-excitation produces prompt X-rays that can be clearly distinguished from the delayed X-rays that follow the transfer of the muon from  $\mu^-p$ . With all this in mind, we restrict our consideration to the following subset of processes:

1. thermalization of the muonic hydrogen atoms via elastic scattering of  $\mu^-p$  by  $H_2$  molecules;
2. depolarization of the muonic hydrogen atoms in spin-flip scattering by  $H_2$  molecules;
3. muon transfer from the hydrogen to higher- $Z$  muonic atom;
4. disappearance of the muon by either a muon decay or nuclear muon capture.

### 3.1. Thermalization and depolarization of the muonic hydrogen atoms

Part of the energy released in the cascade de-excitation of  $\mu^-p$  atoms is transformed into kinetic energy of the latter, and the initial energy distribution in the ground  $1s$  state is spread over a broad interval up to the keV range [18, 19, 20], with the para ( $F = 0$ ) and ortho ( $F = 1$ ) spin states populated statistically. A phenomenological distribution of the initial kinetic energy that has given good results in simulations of preceding experiments is the sum of two Maxwellian distribution density, one corresponding to the target gas temperature, and another one with mean energy of 20 eV; it has been used in the present work too. Thermalization and depolarization occur in elastic and spin-flip scattering with

the surrounding hydrogen and higher-Z atoms and molecules. The energy loss in collisions with the light  $\text{H}_2$  is the main mechanism of thermalization, so that the rate of thermalization is little sensitive to the admixture concentration and depends only on the hydrogen density  $\phi$  (or pressure  $P$ ) and — through the molecular cross sections — on the temperature  $T$ . The same holds for the rate of depolarization.

The process of thermalization is best illustrated with the time evolution of the average kinetic energy of  $(\mu^-p)_{1s}$ ,  $\bar{E}(t; P, T)$ . Figure 1 presents the Monte Carlo simulations for  $\bar{E}(t; P, T)$  in pure hydrogen for a set of relevant pressures  $P$ , at  $T = 300$  K. The plot clearly shows that the time needed

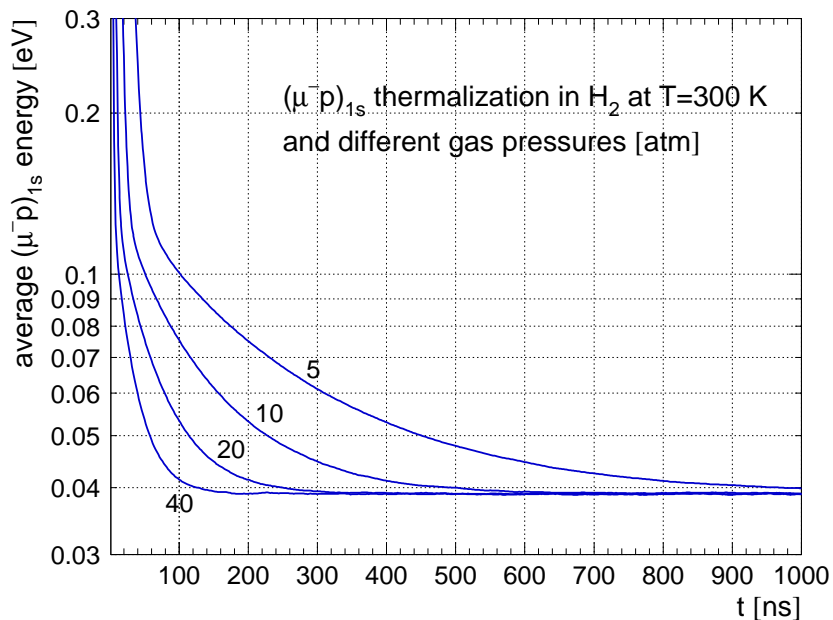


Figure 1: The average  $(\mu^-p)_{1s}$  energy  $\bar{E}(t; P, T)$  versus time  $t$ , for pressures  $P = 5, 10, 20$ , and  $40$  atm (0.51, 1.01, 2.03, and 4.05 MPa).

for the average energy  $\bar{E}(t; P, T)$  to approach the equilibrium energy is approximately inverse proportional to the pressure (i.e., density):  $\bar{E}(t; kP, T) \sim \bar{E}(t/k; P, T)$ ,  $k > 0$ . In particular, at room temperature and 20 atm, the  $(\mu^-p)_{1s}$  atoms are “practically” thermalized already at  $t = 300$  ns. This conclusion is confirmed by the plots in Fig. 2 of  $\bar{E}(t; P, T)$  at fixed pressure, for a set of values of the temperature and the corresponding hydrogen density  $\phi$ , in the units of liquid hydrogen density (LHD). When the density is fixed, the thermalization time is practically the same for all discussed temperatures, which is shown in Fig. 3. At  $\phi = 0.045$ , the  $(\mu^-p)_{1s}$  atoms are thermalized after about 150 ns, for all the temperatures. For times  $5 \text{ ns} \lesssim t \lesssim 150 \text{ ns}$ , the time evolution of energy differs due to the different thermal energies of  $\text{H}_2$  molecules. Thus, the gas density is the parameter that determines the thermalization time at small

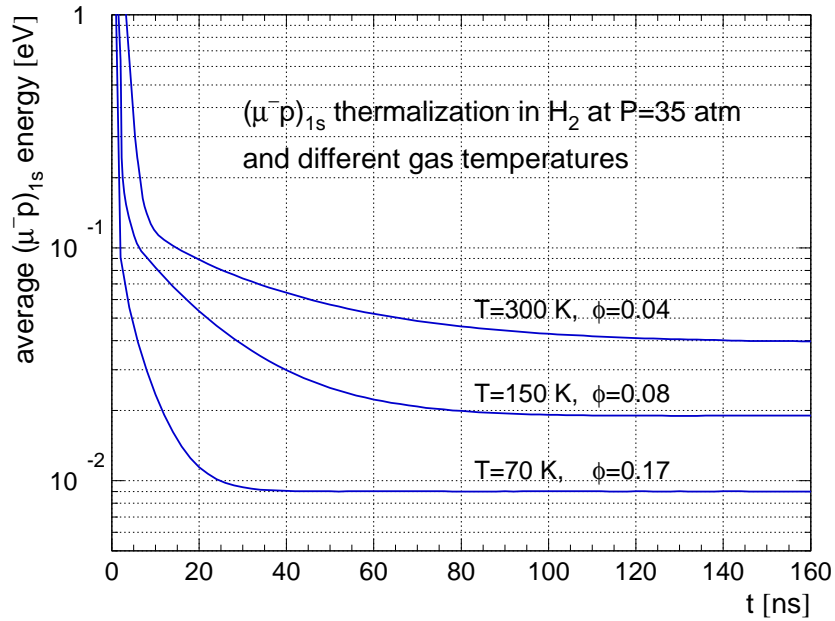


Figure 2: Time evolution of the average  $(\mu^-p)_{1s}$  energy  $\bar{E}(t; P, T)$  at a fixed pressure  $P = 35$  atm (3.55 MPa), for a set of temperatures  $T$ .  $\phi$  is the  $H_2$  gas density in units of LHD.

admixtures of higher- $Z$  gases. The same conclusion can be drawn for the time of quenching the  $F = 1$  state, since the collisions of  $(\mu^-p)_{1s}$  atoms with  $H_2$  molecules establish an effective mechanism of the downwards spin flip.

The  $(\mu^-p)_{1s}$  atom depolarization (i.e., the de-population of the ortho  $F = 1$  spin state) proves to be much faster than the thermalization process: the plot in Fig. 4 of the time evolution of  $Q_{F=1}(t; P, T)$ , the part of all  $(\mu^-p)_{1s}$  atoms that occupy the ortho  $F = 1$  hyperfine level of the ground state (normalized by  $Q_{F=1}(0; P, T) = 3/4$ ), vanishes — at the same temperature and pressure as in Fig. 1 — an order of magnitude faster than the atoms are thermalized. By summarizing the results of the above simulations, we conclude that to a good accuracy one can assume that the muonic hydrogen atoms are completely thermalized and depolarized after  $t_0$  nanoseconds, where the rough estimate of  $t_0$  reads:

$$t_0[\text{ns}] \sim 20 \times T[\text{K}] / P[\text{atm}]. \quad (1)$$

### 3.2. Muon decay and nuclear muon capture

The proposed experimental method consists in measurements of the rate of muon transfer from thermalized  $(\mu^-p)_{1s}$  atoms at time  $t > t_0$ ; the muons that have decayed or been captured by this time are lost. The part of “lost muons” is  $(1 - \exp(-\lambda^* t_0)) / \lambda^*$ ,  $\lambda^* = \lambda_{\text{dec}} + \lambda_{\text{cap}}$  where  $\lambda_{\text{dec}} = 0.45 \mu\text{s}^{-1}$  and  $\lambda_{\text{cap}} = 0.7 \text{ms}^{-1}$  are the free muon decay rate and the nuclear muon capture rate

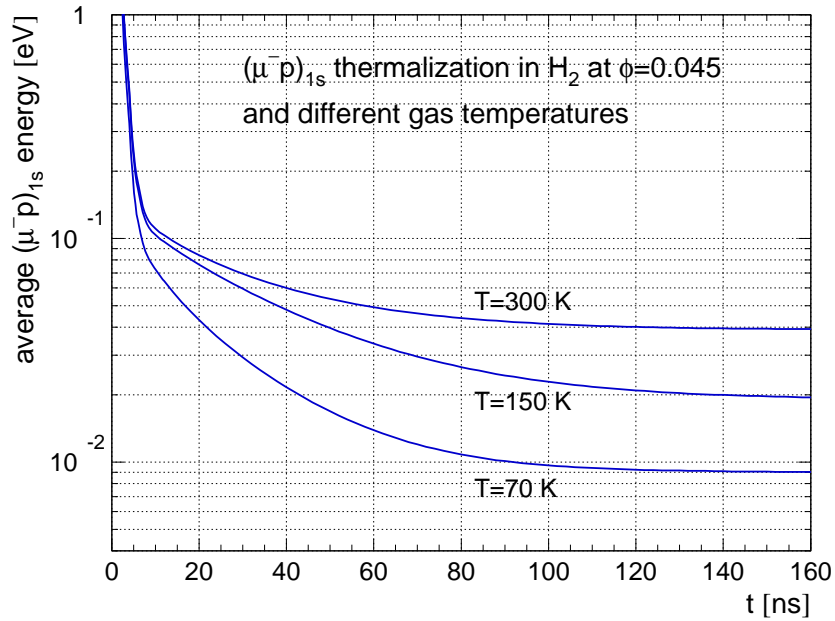


Figure 3: Time evolution of the mean  $\langle \mu^- p \rangle_{1s}$  energy  $\bar{E}(t; \phi, T)$  at a fixed density  $\phi = 0.45$  in units of LHD, for a set of temperatures  $T$ .

in  $\langle \mu^- p \rangle_{1s}$ , both of them — independent of hydrogen gas density or temperature. For  $t_0 = 500$  ns, the losses are  $\sim 20\%$  and increase with  $t_0$ .

### 3.3. Muon transfer to higher-Z muonic atoms

In the experiment for the measurement of the energy dependence of the rate of muon transfer to a higher-Z admixture nucleus we have the following parameters at our disposal to control the processes: the pressure and temperature of the target, the start-of-counting time  $t_0$  and the concentration  $c$  of the admixture, defined as  $c = n_Z / (n_H + n_Z)$ , where  $n_H$  and  $n_Z$  are the number concentrations, i.e. the number of species (atoms or molecules) of hydrogen and higher-Z element per cubic centimeter. The choice of optimal values of these parameters should guarantee that the maximal number of muon transfer events take place from thermalized  $\langle \mu^- p \rangle_{1s}$  atoms.

The Monte Carlo simulations may have, in principle, only restricted validity because for most of the possible admixture gases only the average muon transfer rate is known. Oxygen is one of the very few elements for which there exist experimental and theoretical data about the energy dependence of the transfer rate. We chose to present the results of the simulations for a mixture of hydrogen and oxygen for this reason, and also because it will be the primary target of the oncoming experimental investigations.

In the experiment, it is crucial to have a large number  $\langle \mu^- p \rangle_{1s}$  atoms at times much larger than the time width of the prompt peak. In order to study this

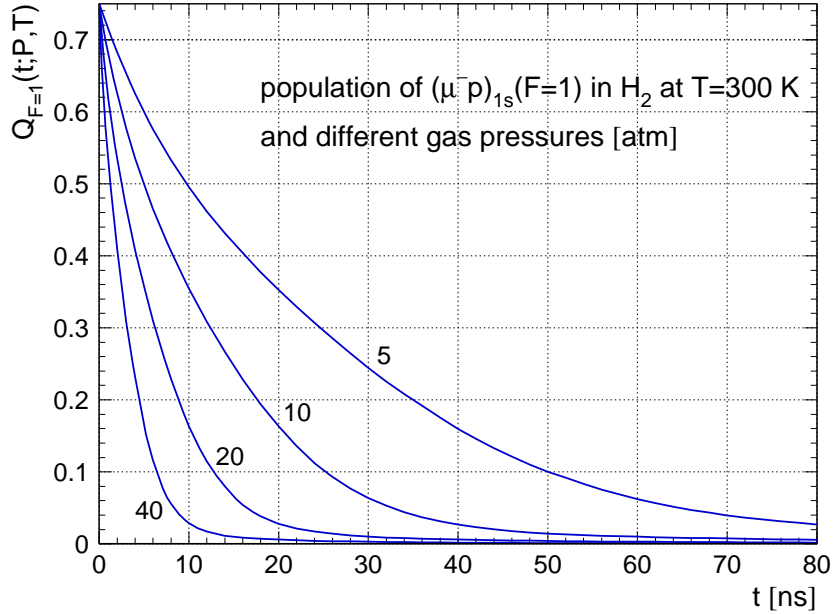


Figure 4: Time evolution of the population  $Q_{F=1}(t; P, T)$  of the  $F = 1$  state in hydrogen at room temperature  $T = 300$  K, for a set of pressures  $P = 5, 10, 20,$  and  $40$  atm (0.51, 1.01, 2.03, and 4.05 MPa).

problem, the Monte Carlo simulations have been performed for a fixed temperature and pressure of  $\text{H}_2 + \text{O}_2$  mixture and various oxygen concentrations. Figure 5 shows the time evolution of the relative population of  $(\mu^- p)_{1s}$  atoms at  $T = 300$  K and  $P = 35$  atm. The curve for  $c = 0\%$ , i.e. for pure  $\text{H}_2$ , determines the absolute upper limit on the number of surviving  $(\mu^- p)_{1s}$  determined by the decay and capture rate  $\lambda^*$ . Any admixture of oxygen decreases this number. At  $c \gtrsim 1\%$ , the hydrogen muonic atoms disappear before thermalization. Simulations with the FLUKA code [21] for various oxygen concentrations at  $P = 35$  atm and  $T = 300$  K have shown that the fraction of muon stops in target practically does not depend on the concentration if  $c \lesssim 1\%$ . The optimal oxygen concentration is the one that provides a maximal number of muon transfer events from *thermalized*  $(\mu^- p)_{1s}$  out of a fixed number of muon stops in  $\text{H}_2$ . The results of the Monte Carlo simulations for various oxygen concentrations at fixed temperature and pressure, shown in Fig. 6, clearly demonstrate that the statistical uncertainty of the experimental data on the muon transfer rate — which is inverse proportional to the squared root of the transfer events — may be drastically reduced by careful planning of the experiment. Our Monte Carlo prediction of the sharp dependence of the number of muon transfer events on the concentration of oxygen, which should be recalculated for any other target temperature and gas admixture, is a central result of the present paper.



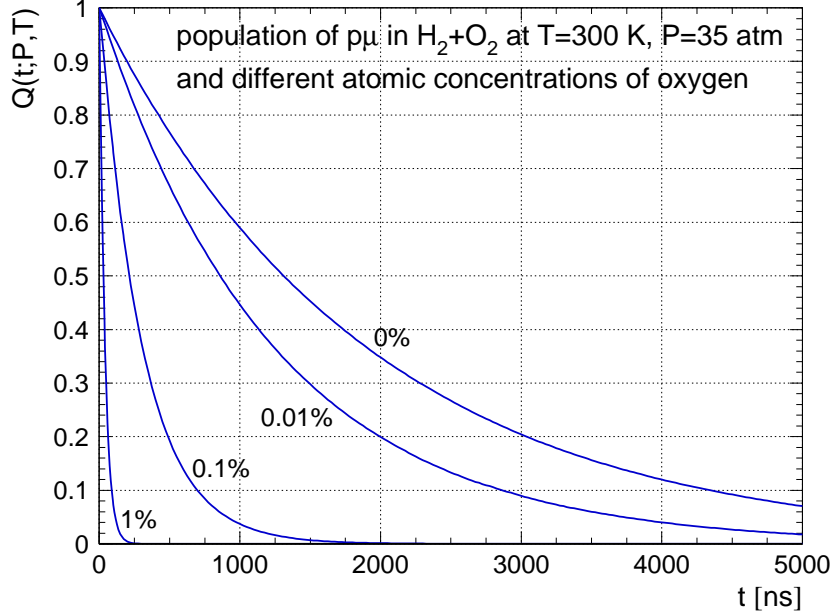


Figure 5: Number  $Q(t; P, T)$  of the  $(\mu^- p)_{1s}$  that have survived in  $H_2+O_2$  mixture at  $T = 300$  K,  $P = 35$  atm (3.55 MPa), and oxygen concentrations  $c = 0\%$ ,  $0.01\%$ ,  $0.1\%$ , and  $1\%$  up to time  $t$ .  $Q(t; P, T)$  is normalized to the number of thermalized depolarized  $(\mu^- p)_{1s}$  atoms at time  $t_0$ . (Here for simplicity we have set  $t_0 = 0$ ).

#### 4. Determining the energy dependence of the muon transfer rate from experimental data

In this last section we present the mathematical model of the proposed experiment and derive the equations that allow for determining the energy dependence of the muon transfer rate from the experimental data on the temperature dependence of the muon transfer rate in thermalized mixture of hydrogen and a higher-Z gas. We consider the general case when the rate  $\lambda$  of muon transfer in collisions of the muonic hydrogen atom with an atom of the heavier admixture does depend on the center-of-mass (CM) collision energy  $\varepsilon$  of the species:  $\lambda = \lambda(\varepsilon)$ . The observable rate of muon transfer  $\Lambda_o$  is the average of  $\lambda$  over the thermal distribution of the collision energy  $\rho(\varepsilon)$ :

$$\Lambda_o = \int \lambda(\varepsilon)\rho(\varepsilon) d\varepsilon.$$

In thermal equilibrium the distribution  $\rho(\varepsilon)$  is nothing but the Maxwell-Boltzmann distribution:

$$\rho(\varepsilon) = \rho_{MB}(\varepsilon; T) = \frac{1}{\varepsilon_T} \rho_0(\varepsilon/\varepsilon_T),$$

$$\rho_0(x) = \frac{2}{\sqrt{\pi}} \sqrt{x} \exp(-x), \quad \varepsilon_T = k_B T,$$

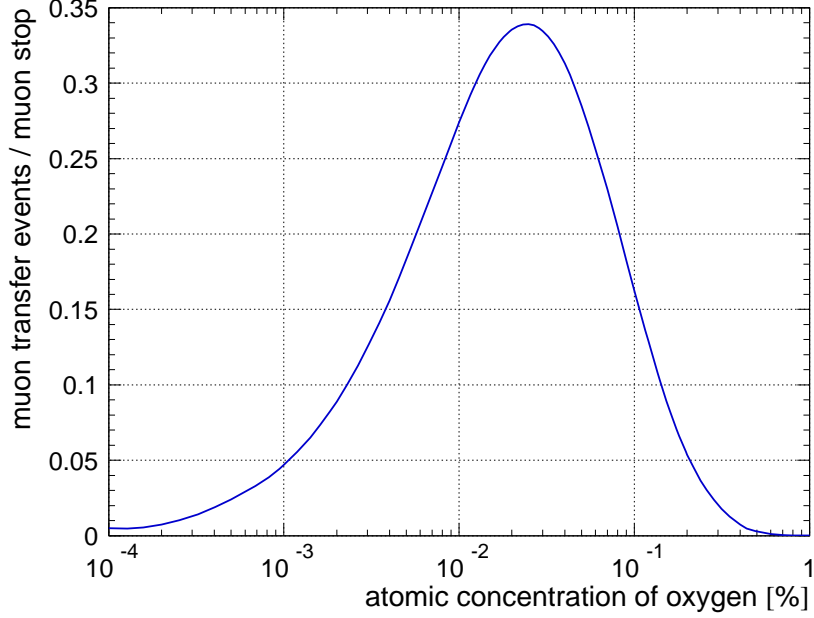


Figure 6: The number of muon transfer events from thermalized  $(\mu^-p)_{1s}$  in  $\text{H}_2$  at  $T = 300$  K and  $P = 35$  atm, normalized to the number of thermalized and depolarized muonic hydrogen atoms at  $t = t_0 = 0$  versus the number concentration  $c$  of oxygen.

where  $T$  is the temperature and  $k_B$  is Boltzmann's constant.

Of primary importance is the behavior of  $\lambda(\varepsilon)$  in the thermal and near-epithermal energy range since the efficiency of the adopted experimental method for the measurement of the  $\mu^-p$  hyperfine splitting depends on the variations of  $\lambda(\varepsilon)$  in this range [3]. We use a polynomial approximation for  $\lambda(\varepsilon)$ :

$$\lambda(\varepsilon) = \sum_{i=1}^{N_a} \lambda_i \prod_{j=1, j \neq i}^{N_a} \frac{\varepsilon - \varepsilon_j}{\varepsilon_i - \varepsilon_j}, \quad \lambda_i = \lambda(\varepsilon_i), \quad (2)$$

where the values  $\varepsilon_i, i = 1, \dots, N_a$  will be referred to as “reference energies”. As long as the transfer rate  $\lambda(\varepsilon)$  is not expected to have any anomalous behavior outside the above range (e.g., abrupt decrease or growth at higher energies) we evaluate the integral for the observable muon transfer rate at temperature  $T$  with a Gauss-type quadrature of appropriate rank  $N_G$ :

$$\Lambda(T) = \int \lambda(\varepsilon) \rho(\varepsilon; T) d\varepsilon = \int \rho_0(x) \lambda(\varepsilon_T x) dx = \sum_{n=1}^{N_G} w_n \lambda(\varepsilon_T x_n), \quad (3)$$

where  $w_n$  and  $x_n$  are the weights and nodes of the Gauss quadrature formula with weight function  $\rho_0(x)$ . Eqs. (2,3) establish a linear relation between  $\Lambda(T)$

and the values  $\lambda_i$ :

$$\Lambda(T) = \sum_{n=1}^{N_G} w_n \sum_{i=1}^{N_a} \prod_{j=1, j \neq i}^{N_a} \frac{k_B T x_n - \varepsilon_j}{\varepsilon_i - \varepsilon_j} \lambda_i. \quad (4)$$

This way, by measuring the values of the observable muon transfer rate  $\Lambda_k = \Lambda(T_k)$  in thermalized target gas at temperatures  $T_k, k = 1, \dots, N_a$ , one will get a system of  $N_a$  linear equations

$$\Lambda_k = \sum_{i=1}^{N_a} M_{ki} \lambda_i, \quad M_{ki} = \sum_{n=1}^{N_G} w_n \prod_{j \neq i} \frac{k_B T_k x_n - \varepsilon_j}{\varepsilon_i - \varepsilon_j}. \quad (5)$$

These equations can be resolved for the values  $\lambda_i$  of the transfer rate at the reference energies:  $\lambda_i = \sum_{k=1}^{N_a} M_{ik}^{-1} \Lambda_k$ , and thus the parameters in the polynomial approximation for  $\lambda(\varepsilon)$  of Eq. (2) are expressed in terms of the experimental data  $\{\Lambda_k\}$ :

$$\lambda(\varepsilon) = \sum_{i=1}^{N_a} \prod_{j=1, j \neq i}^{N_a} \frac{\varepsilon - \varepsilon_j}{\varepsilon_i - \varepsilon_j} \cdot \sum_{k=1}^{N_a} M_{ik}^{-1} \Lambda_k \quad (6)$$

While these transformations are quite straightforward, it is worth briefly discussing the uncertainty of the parameters  $\lambda_i = \lambda(\varepsilon_i)$ , induced by the experimental uncertainty of  $\Lambda_k = \Lambda(T_k)$ . If assuming that  $\Lambda_k$  are normally distributed around  $\bar{\Lambda}_k$  with standard deviation  $\Delta_k$ , the parameters  $\lambda_i$  will be normally distributed with standard deviation  $\delta_i$ , where

$$\delta_i^2 = \sum_{k=1}^{N_a} (M_{ik}^{-1})^2 \Delta_k^2. \quad (7)$$

The specific values of  $\delta_i$  depend on the choice of target temperatures ( $T_k, k = 1, \dots, N_a$ ) (that may be predetermined by the available cooling devices) and of the reference energies  $\varepsilon_i$  (whose optimal choice will be done after simulations of the muonic hydrogen HFS experiment). Consider as an example a series of three measurements at 70 K (cooling with liquid nitrogen), 195 K (liquid carbon dioxide) and 300 K (room temperature), and the set of reference energies  $\varepsilon_1 = 0.006$  eV,  $\varepsilon_2 = 0.05$  eV, and  $\varepsilon_3 = 0.12$  eV. For simplicity, we assume that all experimental uncertainties are equal:  $\Delta_k = \Delta, k = 1, \dots, 3$ . The accuracy of the proposed method is assessed with the ratios  $\delta_i/\Delta$  that show how much the uncertainties of the calculated values  $\lambda_i$  exceed the uncertainty of the experimental data  $\Lambda_k$ . On Fig. 7 we plot (with thick solid curves) the response of  $\delta_i/\Delta$  to the variations of each of the three reference energies  $\varepsilon_j, j = 1, 2, 3$ , in the neighborhood of the values listed above (denoted with dashed vertical lines) while keeping the other two fixed. We see that:

- the uncertainty of  $\lambda(\varepsilon)$  increases very fast with the reference energy  $\varepsilon$ . This is not surprising: the contribution to the observable transfer rate  $\Lambda(T)$  from the “code” of the Maxwell-Boltzman distribution  $\rho_{\text{MB}}(\varepsilon; T)$  (plotted with dotted lines for the selected temperatures  $T_k$ ) decreases exponentially with energy;
- the uncertainty  $\delta_i$  is little sensitive to variations of the reference energies  $\varepsilon_j, j \neq i$ .

Eq. 7 allows for estimating the accuracy goals  $\Delta_k$  in the measurements of  $\Lambda_k$  that will lead to uncertainties  $\delta_i$  of the calculated muon transfer rates  $\lambda_i$  within the limits, required for planning and optimizing the muonic hydrogen HFS experiment [3]. The example discussed above shows that, with a relatively modest statistics of  $\sim 10^6$  muon transfer events, the transfer rate  $\lambda(\varepsilon)$  can be determined in the whole range of epithermal energies of interest with uncertainty of the order of 1% – far below the uncertainty of the currently available data about the energy dependence of the muon transfer rates.

The numerical results are independent of the rank  $N_G$  of the Gauss quadrature formulae provided that  $N_a \leq 2N_g$ . The nodes and weights of two lower rank quadratures are given in Table 1.

Table 1: Examples of quadrature formula for averaging over the Maxwell-Boltzmann energy distribution

$N_g$	Nodes $x_n$	Weights $w_n$
3	0.666326	0.6400012
	2.800775	0.3445751
	7.032899	0.0154237
5	0.431399	0.4180087
	1.759754	0.4655516
	4.104465	0.1103327
	7.746704	0.00606325
	13.45768	0.00004372

## 5. Conclusions

Using a realistic model of the processes with muonic hydrogen atoms in the ground state that occur in mixture of hydrogen and a higher-Z gas, we have found by means of Monte Carlo simulations the experimental conditions (admixture concentration and time gate) for preselected pressure and temperature which optimize the efficiency of the measurement of the temperature dependence of the average rate of muon transfer from muonic hydrogen to the higher-Z admixture. We have also developed a computational technique allowing to determine from these data the energy dependence of the muon transfer rate and give an estimate of the experimental uncertainty of the latter. These results will be implemented in the methodology of the oncoming experiment FAMU [23], to be performed in 2015 at the RIKEN-RAL muon facility.

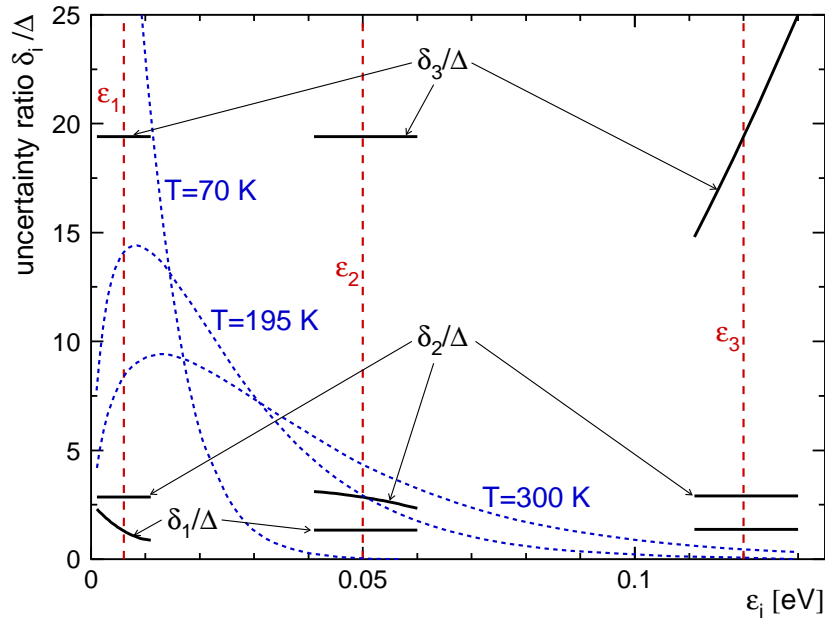


Figure 7: Dependence of the uncertainty ratios  $\delta_i/\Delta$  on the reference energies  $\varepsilon_j$ ,  $j = 1, 2, 3$ . The thick solid piecewise curves display the response of  $\delta_i/\Delta$  to variations of  $\varepsilon_j$  in the neighborhood of the value denoted by a dashed vertical line while keeping fixed the other two reference energies  $\varepsilon_k$ ,  $k \neq j$ . The dotted curves are the Maxwell-Boltzmann energy distribution densities for temperatures  $T = 70$  K, 195 K, and 300 K.

## Acknowledgments

This work has been partly supported under the bilateral agreement of the Bulgarian Academy of sciences and the Polish Academy of Sciences.

## References

### References

- [1] D. Bakalov, E. Milotti, C. Rizzo et al., Phys. Lett. A 172 (1993) 277.
- [2] H. Heliwig, R. F. C. Vessot, M. W. Levine et al., IEEE Trans. Instrum. Meas. IM-19 (1970) 200; L. Essen, R. W. Donaldson, M. J. Bangham, E. G. Hope, Nature 229 (1971) 110; M. J. Bangham, R. W. Donaldson, NPL Report Qu 17 (March 1971).
- [3] A. Adamczak, D. Bakalov, K. Bakalova et al., Hyperfine Interact. 136 (2001) 1.
- [4] A. Antognini, K. Schuhmann, F. D. Amaro et al., IEEE J. Quant. Electr. 45 (2009) 993; A. Vacchi, A. Adamczak, B. Andreson et al., SPIE Newsroom 10.1117/2.1201207.004274 (2012).

- [5] R. Pohl, A. Antognini, F. Nez et al., *Nature* 466 (2010) 213.
- [6] F. Mulhauser, H. Schneuwly, *Hyperfine Interact.* 82 (1993) 507.
- [7] R. Jacot-Guillarmod, F. Mulhauser, C. Piller, H. Schneuwly, *Phys. Rev. Lett.* 65 (1990) 709.
- [8] R. Jacot-Guillarmod, F. Mulhauser, C. Piller et al., *Phys. Rev. A* 55 (1997) 3447.
- [9] A. Adamczak, M. P. Faifman, L. I. Ponomarev et al., *At. Data Nucl. Data Tables* 62 (1996) 255.
- [10] A. Adamczak, *Phys. Rev. A* 74 (2006) 042718.
- [11] A. Werthmüller, A. Adamczak, R. Jacot-Guillarmod et al., *Hyperfine Interact.* 116 (1998) 1.
- [12] A. Adamczak, J. Gronowski, *Eur. Phys. J. D* 41 (2007) 493.
- [13] V. A. Andreev, T. I. Banks, R. M. Carey et al., *Phys. Rev. Lett.* 110 (2013) 012504.
- [14] M. P. Faifman, *Muon Catalyzed Fusion* 4 (1989) 341.
- [15] L. D. Landau and E. M. Lifshitz, *Quantum Mechanics* (Pergamon, Oxford, 1977), p.601.
- [16] S. S. Gershtein, *Zh. Exp. Teor. Fiz.* 43 (1962) 706 [*Sov. Phys. JETP* 16 (1963) 50].
- [17] A. Dupays, B. Lepetit, J. A. Beswick et al., *Phys. Rev. A* 69 (2004) 062501.
- [18] T. S. Jensen, V. E. Markushin, *Eur. Phys. J. D* 21 (2002) 271.
- [19] R. Pohl, H. Daniel, F. J. Hartmann et al., *Phys. Rev. Lett.* 97 (2006) 193402.
- [20] M. P. Faifman, L. I. Men'shikov, *Proceedings of the International Conference on Muon Catalyzed Fusion and Related Topics ( $\mu$ CF-07)*, JINR, Dubna, 2008, p. 233.
- [21] A. Ferrari, P. R. Sala, A. Fasso, J. Ranft, *SLAC-R-773* (2005).
- [22] A. Adamczak, C. Chiccoli, V. I. Korobov et al., *Phys. Lett. B* 285 (1992) 319.
- [23] <http://webint.ts.infn.it/en/research/exp/famu.html>.